

Kinetics of Solid-State Synthesis of Quaternary $\text{Cu}_2\text{FeSnS}_4$ (Stannite) Nanocrystals for Solar Energy Applications

P. BALÁŽ^{a,*}, M. BALÁŽ^a, A. ZORKOVSKÁ^a, I. ŠKORVÁNEK^b, Z. BUJŇÁKOVÁ^a AND J. TRAJIĆ^c

^aInstitute of Geotechnics of Slovak Academy of Sciences, Watsonova 45, 04001 Košice, Slovakia

^bInstitute of Experimental Physics of Slovak Academy of Sciences, Watsonova 47, 04353 Košice, Slovakia

^cInstitute of Physics Belgrade, Pregrevica 118, 11080 Belgrade, Serbia

In this study we demonstrate the use of elemental precursors (Cu, Fe, Sn, S) to obtain stannite forms by a solid-state one-pot mechanochemical synthesis. In the processing route, we report the kinetics of the synthesis. For the characterization of the unique nanostructures, X-ray diffraction, specific surface area measurements and SQUID magnetometry methods were applied. CFTS polymorphs with the tetragonal body-centered structure with the average crystallite size 18–19 nm were obtained. The weak ferromagnetic properties of the quaternary nanocrystals after maximum milling time were also documented.

DOI: [10.12693/APhysPolA.131.1153](https://doi.org/10.12693/APhysPolA.131.1153)

PACS/topics: 75.50.Pp, 81.05.Hd, 61.46.Hk

1. Introduction

There is a general paradox in present research and application of chalcogenide solar materials. On one side, $\text{CuIn}_{1-x}\text{Ga}_x\text{Se}_2$ (CIGS) thin film solar cells attracted a big attention owing to their high power conversion efficiency and good stability. On the other side, these materials represent the potential environmental problem because of Se toxicity, In and Ga limited availability and high price [1–4]. Quaternary semiconductor nanocrystals provide promising alternatives to conventional photovoltaic materials because of their environmental acceptance (application of S instead of toxic Se), cheapness and availability (application of earth-abundant Fe, Zn and Sn instead of scarce In and Ga). For example kesterite (CZTS) and stannite (CFTS) possess many advantageous characteristics for photovoltaic applications, such as composition from the abundant and non-toxic elements, suitable band gap, high absorption coefficient and high radiation stability [3, 5, 6].

Stannite $\text{Cu}_2\text{FeSnS}_4$ has been recently prepared by several techniques such as solution-based synthesis, hot injection and microwave irradiation [7–15]. However, these techniques are complex, time-consuming, need high temperature and toxic organic solvents.

In this study, we attempt to synthesize CFTS phase by a novel solid-state reaction using a high-energy planetary milling. The structural, optical and magnetic properties including kinetics of the phase evolution are investigated.

2. Experimental

The solid-state synthesis of CFTS was realized in a planetary mill Pulverisette 6 (Fritsch, Germany) under the following conditions: loading — 50 balls ($d = 10$ mm)

of tungsten carbide, volume of milling pot from tungsten carbide — 250 mL, input mass of sample mixed from Cu, Fe, Sn and S elements in a stoichiometric ratio of $\text{Cu}_2\text{FeSnS}_4$ — 5 g, ball-to-powder ratio — 70, milling speed — 500 min^{-1} , milling time — 1–120 min, milling atmosphere — argon.

The crystal structure was characterized by using a D8 Advance Bruker X-ray diffractometer (Bruker, Germany) in the Bragg–Brentano geometry working with a $\text{Cu } K_\alpha$ radiation ($\lambda = 0.15406$ nm) and a scintillation detector. The data were collected over the angular range $10^\circ < 2\theta < 100^\circ$ with scanning steps of 0.02° and a measurement step time interval of 6 s. For the data processing, the commercial Bruker tools have been used. Specifically, for the phase identification, the *DiffraC^{plus}* Eva and the ICDD PDF2 database were utilized.

For the determination of the elemental sulphur content, the Soxhlet extractor, with CS_2 as the extraction solvent, in which elemental sulphur is dissolved, was used. The non-reacted sulphur present in the extracted CFTS sample remains in the thimble. The amount of the non-reacted sulphur dissolved in CS_2 is calculated from the weight difference of the distillation flask before the experiment and after the evaporation of solvent.

A nitrogen adsorption apparatus NOVA 1200e Surface Area & Pore Size Analyzer (Quantachrome Instruments, United Kingdom) was employed to record the specific surface area (S_{BET}) values, which were calculated using the Brunauer–Emmett–Teller (BET) equation. The measurements were performed at the liquid nitrogen temperature.

The magnetic measurements were performed by a Magnetic Property Measuring System model MPMS-XL-5 (Quantum Design, USA) equipped with 5 T superconducting magnet. The magnetization curves as a function of the applied field have been collected at room temperature.

*corresponding author; e-mail: balaz@saske.sk

3. Results and discussion

3.1. Structural analysis

The XRD patterns of the starting mixture (Cu, Fe, Sn and S powders) milled for 20–120 min are shown in Fig. 1.

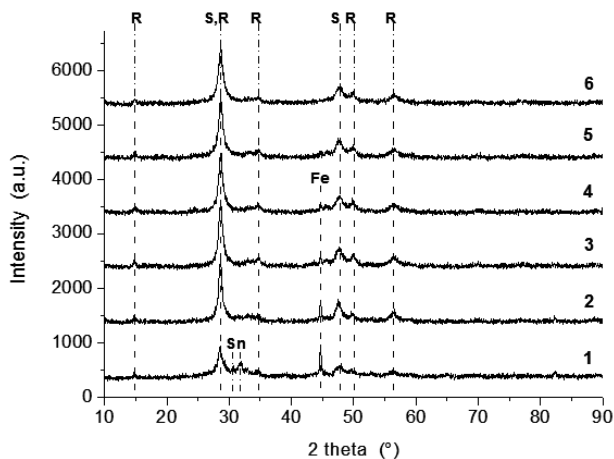
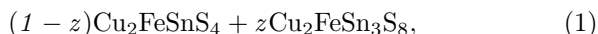
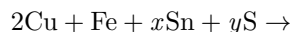


Fig. 1. XRD patterns of the CFTS samples, milling time, t_M : 1 — 20 min, 2 — 30 min, 3 — 45 min, 4 — 60 min, 5 — 90 min, 6 — 120 min; R — rhodostannite $\text{Cu}_2\text{FeSn}_3\text{S}_8$, S — stannite $\text{Cu}_2\text{FeSnS}_4$, Fe — elemental iron, Sn — elemental tin.

In principle, the mechanochemical synthesis can be described by a hypothetical Eq. (1):



where $x = 1$ and 3 ; $y = 4$ and 8 for stannite and rhodostannite formation, respectively, and $z = 0 \div 1$. At the beginning of the mechanochemical synthesis, the peaks of the non-reacted Sn and Fe precursors can be traced (plot 1). However, with the progress of reaction, only the peaks of the non-consumed Fe are visible (plots 2–4). Later on, only the peaks corresponding to stannite $\text{Cu}_2\text{FeSnS}_4$ (S, JCPDS 44-1476) and rhodostannite $\text{Cu}_2\text{FeSn}_3\text{S}_8$ (R, JCPDS 85-0378) are visible (plots 5,6). In this case, the observed peaks can be assigned to the (112), (204) and (312) planes of the tetragonal crystals. Both tetragonal phases show the presence of crystallites with the sizes calculated by the Rietveld analysis 18.3 nm and 18.9 nm for stannite and rhodostannite, respectively. The new phenomenon of stannite \rightarrow rhodostannite transformation can be traced as a consequence of milling (Fig. 2).

The amounts 76% stannite and 24% rhodostannite have been calculated for the sample milled for 120 min (Fig. 1, plot 6). In nature, rhodostannite is a replacement product of stannite [16]. This transformation may happen also with synthetic crystals by the application of high-energy milling, which often leads to the products with extraordinary properties [17]. As stated in [18], high local pressures and contact surface of the milled solids,

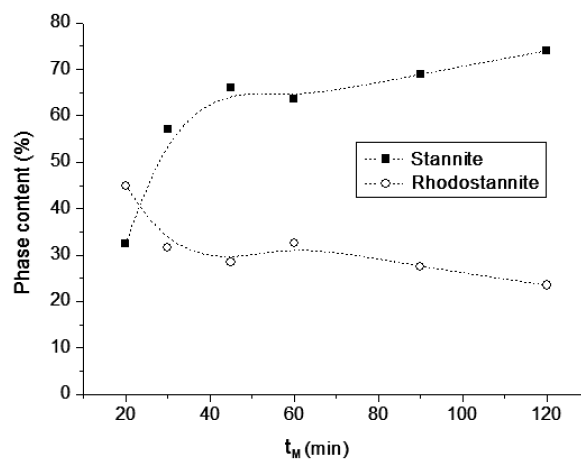
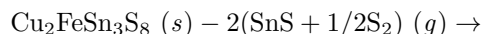


Fig. 2. Stannite, $\text{Cu}_2\text{FeSnS}_4 \rightarrow$ rhodostannite, $\text{Cu}_2\text{FeSn}_3\text{S}_8$ transformation in dependence on milling time, t_M .

as well as volume defects (e.g. strain) are responsible for such transformations. We speculate that during milling, SnS and S_2 are liberated from rhodostannite, according to a hypothetical Eq. (2):



This is supported by findings in [19], where SnS as volatile compound, in which tin is present as Sn(II) ion, is formed from kesterite structure, and, together with sulphur, is liberated into gas phase.

The kinetics of the solid-state reaction of Cu, Fe, Sn and S elements yielding quaternary nanocrystals is depicted in Fig. 3.

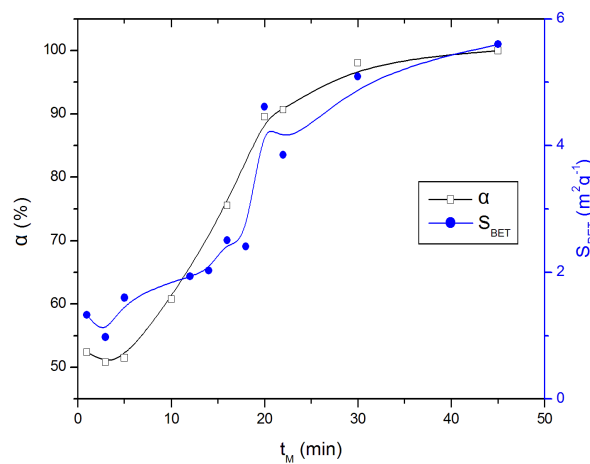


Fig. 3. Conversion degree of reaction, α and specific surface area, S_{BET} vs. milling time, t_M .

The Soxhlet method (see Sect. 2), by which the amount of non-consumed sulphur, as a measure of the progress of the mechanochemical synthesis, can be determined, has been applied for the determination of the conversion degree, α . The synthesis is very fast and the values

$\alpha \approx 50\%$ can be obtained right few moments after its initiation. A sigmoidal shape of $\alpha(t_M)$ dependence proves the acceleration of the synthesis at $t_M \approx 15$ min. Later on, the reaction does not proceed less quickly and at $t_M \geq 45$ min, practically no non-reacted sulphur has been detected, which means its total consumption with full conversion of the precursors to stannite polymorphs. The synthesis reaction (2) is topochemical, which is supported by the very similar course of $S_{\text{BET}}(t_M)$ plot, which hints to the decisive role of the surface defects created during the synthesis.

3.2. Magnetic properties

Figure 4 shows that the magnetization values for $M(H)$ curves taken at 300 K are well-saturated after the application of magnetic fields with the magnitude higher than 1 T. In principle, the magnetic data can also be used for progress evaluation of reaction (2). The final products of this reaction, namely stannite and rhodostannite, are weak magnetic (paramagnetic) substances at a room temperature [11, 20]. Therefore, the differences in the saturation magnetization of the samples milled for different times are caused mainly by the different amount of the non-consumed iron, which is the only ferromagnetic component in these materials at 300 K. For longer milling times, the saturation magnetization rapidly decreases, indicating that significant amount of elemental Fe has been already consumed by the mechanochemical reaction.

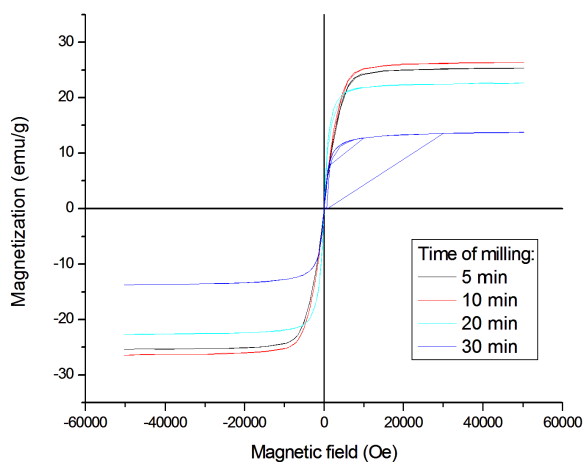


Fig. 4. Magnetization vs. magnetic field for the CFTS samples milled for different times.

4. Conclusions

The simple one-pot solid-state synthesis of CFTS quaternary nanocrystals with the properties suitable for the application in solar cell materials has been demonstrated. Stannite, $\text{Cu}_2\text{FeSnS}_4$ and rhodostannite, $\text{Cu}_2\text{FeSn}_3\text{S}_8$ with crystallite sizes 18–19 nm were obtained. The influence of mechanical treatment is manifested by stannite-rhodostannite transformation. The

newly revealed phenomena broaden the scope of quaternary nanocrystals application.

Acknowledgments

This work was supported by the Slovak Research and Development Agency (project APVV-0103-14) and the Slovak Grant Agency VEGA (projects 2/0027/14 and 1/0377/16). The support of European project COST (OC-2015-1-19345) is also acknowledged.

References

- [1] W. Hsu, C.M. Sutter-Fella, M. Hettick, L.T. Cheng, S.W. Chan, Y.F. Chen, Y.P. Zeng, M. Zheng, H.P. Wang, C.C. Chiang, A. Javey, *Sci. Rep.* **5**, (2015).
- [2] Q. Guo, G.M. Ford, W.C. Yang, B.C. Walker, E.A. Stach, H.W. Hillhouse, R. Agrawal, *J. Am. Chem. Soc.* **132**, 17384 (2010).
- [3] S. Delbos, *EPJ Photovolt.* **3**, 35004 (2012).
- [4] X.B. Song, X. Ji, M. Li, W.D. Lin, X. Luo, H. Zhang, *Int. J. Photoenergy* 613173 (2014).
- [5] J.J. Scragg, *Copper Zinc Tin Sulfide Thin Films for Photovoltaics*, Springer-Verlag, Berlin 2011.
- [6] S. Siebentritt, S. Schorr, *Prog. Photovolt.* **20**, 512 (2012).
- [7] L.H. Ai, J. Jiang, *Nanotechnology* **23**, 495601 (2012).
- [8] W. Wang, H.L. Shen, H.Y. Yao, J.Z. Li, *Mater. Lett.* **125**, 183 (2014).
- [9] M. Cao, C. Li, B.L. Zhang, J. Huang, L.J. Wang, Y. Shen, *J. Alloys Comp.* **622**, 695 (2015).
- [10] C. Li, M. Cao, J. Huang, L.J. Wang, Y. Shen, *Mater. Sci. Semicond. Process.* **31**, 287 (2015).
- [11] Y. Cui, R.P. Deng, G. Wang, D.C. Pan, *J. Mater. Chem.* **22**, 23136 (2012).
- [12] X.K. Meng, H.M. Deng, J. He, L. Sun, P.X. Yang, J.H. Chu, *Mater. Lett.* **151**, 61 (2015).
- [13] C. Huang, Y. Chan, F.Y. Liu, D. Tang, J. Yang, Y.Q. Lai, J. Li, Y.X. Liu, *J. Mater. Chem. A* **1**, 5402 (2013).
- [14] C. Yan, C. Huang, J. Yang, F.Y. Liu, J. Liu, Y.Q. Lai, J. Li, Y.X. Liu, *Chem. Commun.* **48**, 2603 (2012).
- [15] B.B. Zhou, X.N. Yan, P. Li, L.B. Yang, D.Y. Yu, *Eur. J. Inorg. Chem.* **2015**, 2690 (2015).
- [16] H. Hey, *Mineral. Mag.* **37**, 954 (1970).
- [17] P. Baláž, M. Achimovičová, M. Baláž, P. Billik, Z. Cherkezova-Zheleva, J.M. Criado, F. Delogu, E. Dutková, E. Gaffet, F.J. Gotor, R. Kumar, I. Mitov, T. Rojac, M. Senna, A. Streletskii, K. Wiczorek-Ciurawa, *Chem. Soc. Rev.* **42**, 7571 (2013).
- [18] E.G. Avvakumov, *Methods in Chemical Processes Activation*, Nauka, Novosibirsk 1979.
- [19] J.J. Scragg, T. Ericson, T. Kubart, M. Edoff, C. Platzer-Bjorkman, *Chem. Mater.* **23**, 4625 (2011).
- [20] M. Womes, J.C. Jumas, J. Olivierfourcade, F. Aubertin, U. Gonser, *Chem. Phys. Lett.* **201**, 555 (1993).